EARTH SURFACE PROCESSES AND LANDFORMS
Earth Surf. Process. Landforms **42**, 460–472 (2017)

Published online 30 August 2016 in Wiley Online Library
(wileyonlinelibrary.com) DOI: 10.1002/esp.4002

Controls on the occurrence and prevalence of floodplain channels in meandering rivers

Scott R. David,[1,2]* Douglas A. Edmonds[1,2] and Sally L. Letsinger[2]
[1] Department of Geological Sciences, Indiana University, Bloomington, IN USA
[2] Center for Geospatial Data Analysis, Indiana Geological Survey, Indiana University, Bloomington, IN USA

Received 19 February 2016; Revised 6 July 2016; Accepted 7 July 2016

*Correspondence to: Scott R. David, Department of Geological Sciences, Indiana University, Bloomington, IN 47401, USA. E-mail: davids@indiana.edu

ESPL
Earth Surface Processes and Landforms

ABSTRACT: The process of channelization on river floodplains plays an essential role in regulating river sinuosity and creating river avulsions. Most channelization occurs within the channel belt (e.g. chute channels), but growing evidence suggests some channels originate outside of the channel-belt in the floodplain. To understand the occurrence and prevalence of these floodplain channels we mapped 3064 km^2 of floodplain in Indiana, USA using 1.5 m resolution digital elevation models (DEMs) derived from airborne light detection and ranging (LiDAR) data. We find the following range of channelization types on floodplains in Indiana: 6.8% of floodplain area has no evidence of channelization, 55.9% of floodplains show evidence (e.g. oxbow lakes) of chute-channel activity in the channel belt, and 37.3% of floodplains contain floodplain channels that form long, coherent down-valley pathways with bifurcations and confluences, and they are active only during overbank discharge. Whereas the first two types of floodplains are relatively well studied, only a few studies have recognized the existence of floodplain channels. To understand why floodplain channels occur, we compared the presence of channelization types with measured floodplain width, floodplain slope, river width, river meander rate, sinuosity, flooding frequency, soil composition, and land cover. Results show floodplain channels occur when the fluvial systems are characterized by large floodplain-to-river widths, relatively higher meandering rates, and are dominantly used for agriculture. More detailed reach-scale mapping reveals that up to 75% of channel reaches within floodplain channels are likely paleo-meander cutoffs. The meander cutoffs are connected by secondary channels to form floodplain channels. We suggest that secondary channels within floodplains form by differential erosion across the floodplain, linking together pre-existing topographic lows, such as meander cutoffs. Copyright © 2016 John Wiley & Sons, Ltd.

KEYWORDS: floodplain; floodplain channels; morphology; avulsion; LiDAR

Introduction

The formation of channels on river floodplains is a key process for avulsion, crevasse splay dynamics, and the planform dynamics of the main channel. Typically new channel segments are created within the active channel belt (e.g. Hooke, 1995; Gay *et al.*, 1998; Constantine *et al.*, 2014; Harrison *et al.*, 2015). These chute channels are short segments, usually on the order of one meander wavelength, that form across a subaerial surface and link together reaches of the same river. They commonly occur when channels cut across point bars or exposed alluvial bars (Bridge, 2003). Chute channels regulate sinuosity in meandering rivers by reducing total river length (Hooke, 1995; Gay *et al.*, 1998, Camporeale *et al.*, 2005; Zinger *et al.*, 2011), and they facilitate the dynamic transformation of river morphology between meandering and braided (Ashmore, 1991; Braudrick *et al.*, 2009; Grenfell *et al.*, 2012; van Dijk *et al.*, 2012).

Channel segments also form in the floodplain far away from the main channel. We refer to these as floodplain channels because they seemingly differ from chute channels. After all they do not serve to reduce sinuosity of the main channel or create a steeper pathway; rather, floodplain channels form only through overbank and flooding processes and can span multiple meander wavelengths (Mertes *et al.*, 1996; Stølum, 1998, Fagan and Nanson, 2004; Trigg *et al.*, 2012). For instance, Fagan and Nanson (2004) note that floodplain channels are only active at overbank discharge and extend into the floodplain of Copper Creek in Australia. Mertes *et al.* (1996) showed that floodplain channels can extend to the floodplain margin, and can vary from one floodplain channel to multiple interconnected channels. Similar floodplain channels have been found on the Amazon River in Brazil (Mertes *et al.*, 1996; Trigg *et al.*, 2012) and the Kolymar River in Russia (Lewin and Ashworth, 2014).

In this study, we aim to explore the prevalence and occurrence of floodplain channels given that they are relatively understudied compared to chute channels. Here we address the following questions: (1) What hydrologic and morphologic parameters (e.g. floodplain width, river sinuosity, floodplain slope) are associated with the occurrence of floodplain channels?; and (2) How do floodplain channels arise? As a first step towards these ends, we document the hydrologic and morphologic differences between floodplains with and without floodplain channels in Indiana, USA. We find that floodplain channels occur in floodplains that have large floodplain-to-river widths, relatively higher meandering rates, and have predominately agricultural land cover.

Background

Types of floodplain channelization

Floodplains of meandering rivers contain at least two types of channelization (Figure 1). The first type of channelization occurs from chute channels, which originate within the channel-belt (Figure 1A–C). The second type of channelization we refer to generically as floodplain channels (Figure 1D). Here use the term floodplain channels to refer to any channel segment on the floodplain that can operate independently from the dynamics of the main channel. Limited data suggests such floodplain channels arise for floodplain drainage and floodwave conveyance (Fagan and Nanson, 2004; Trigg *et al.*, 2012).

Chute channels

Chute channels create a steeper pathway for the river system and serve to reduce and regulate sinuosity (Camporeale *et al.*, 2005). McGowen and Garner (1970) classically described how chute channels form during flood when the zone of maximum velocity shifts toward the inner bend of the meander and scours a channel through the point bar (Figure 1A). Dunne and Aalto (2013) suggest that these types of chute channels would be favored under conditions with low vertical accretion rates on the alluvial bar, so as not to rapidly infill swales, and long flooding durations with a suspended sediment-poor receding limb that encourage erosion. This process can be influenced by the presence and spacing of scroll and swale bars. These channel chutes help initiate the transition from single thread to multi thread river morphologies. Indeed, experiments by Braudrick *et al.* (2009) showed that when chute channels in these locations were suppressed by fine sediment deposition, sinuous planform morphologies formed.

Chute channels also form from headwardly eroding knickpoints or erosive enlargement of swales (Figure 1B and C). Headwardly eroding chute channels may initiate from a blockage in the river that increases the water level and causes localized overbank flow that plunges back into the river channel initiating headward erosion (Keller and Swanson, 1979; Gay *et al.*, 1998; Thompson, 2003). Keller and Swanson (1979) found that debris jams of dead organic matter (e.g. logs) on small streams in North Carolina, USA formed blockages in the channel, driving overbank flow and the development of a chute channel through headward incision. Embayment enlargement, however, occurs along the channel bank and results from localized bank erosion, usually on the upstream portion of the meander. Constantine *et al.* (2010) observed that embayments on the Sacramento River in California, USA typically form where the channel curvature is greatest in the upstream portion of the meander.

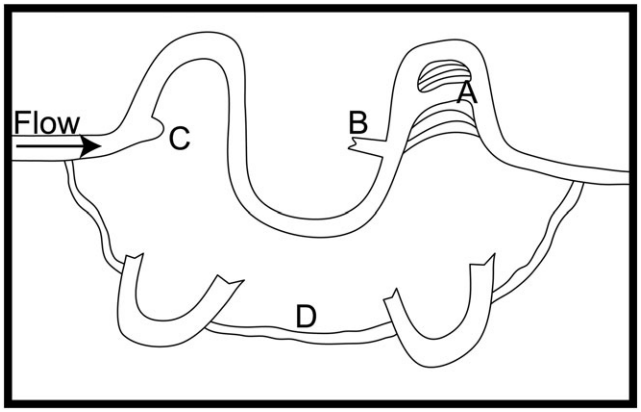

Figure 1. Illustration of different types of floodplain channelization. (A) Chute channels can form from bar dissection, (B) headward incision, and (C) embayment formation. (D) Floodplain channels are not obviously associated with the main channel and extend outward from the active channel belt.

Floodplain channels

Floodplain channels have a variety of attributes that suggest they are different from chute channels. Floodplain channels span many meander wavelengths, they are only active during overbank flow, and do not always connect to different parts of the main channel. The origin and function of floodplain channels to the meandering river system is also unclear. Floodplain channels were first recognized on Copper Creek, Australia, but they were misinterpreted to be relict features of previous braided rivers (Rust, 1981; Rust and Legun, 1983), whereas later work by Fagan and Nanson (2004) identified them to be modern features. Fagan and Nanson (2004) classified floodplain channels, based on planform geometry, into reticulate (or networked) channels or braided channels. Multiple regression analysis suggests floodplain width and transmission losses play an important role in setting the planform geometry of the floodplain channels. Their study proposes a continuum model to predict floodplain channel geometries. The continuum model spans low, moderate, and high overbank flow power and inundation frequency which produce no channels, reticulate floodplain channels, and braided floodplain channel forms, respectively.

A recent study by Trigg *et al.* (2012) describes networks of floodplain channels along the Amazon River. The Trigg *et al.* (2012) study measured width, depth, sinuosity, and length of floodplain channels to provide insight into the hydrological function of these floodplain channels. They hypothesized that floodplain channels that are more deeply incised into the floodplain receive extra flow input from their own local catchments. The increased flow input allows for strong flow reversals creating higher velocities in the floodplain channels as they drain. The increased velocities promote higher erosive potential driving further floodplain channel development. While the Trigg *et al.* (2012) study does provide insight into Amazon River's floodplain channels, it does not address the origin of these channel networks.

Of the types of channelization defined in this paper little is known about the origin and function of floodplain channels. Here we seek to understand their (1) spatial distribution and prevalence; (2) morphometry; and (3) the geomorphic and hydrologic conditions that lead to floodplain channels. Relatively little is known about floodplain channels probably because they were difficult to observe prior to the proliferation of high resolution topographic data, such as LiDAR (light detection and ranging). LiDAR provides unprecedented detail of subtle topography across floodplains. As we will show in this paper, floodplain channels form channel networks with spatially coherent down-valley pathways where individual channel segments have widths ranging from meters to tens of meters. Our study suggests floodplain channels form in floodplains that have actively migrating rivers, large floodplain widths compared to river widths, and high flood frequency. We propose that these channels arise to convey overbank discharge and possibly aid in transitioning fluvial styles from meandering to anabranching. The transition from single to anabranching would occur when a given floodplain channel has incised deep enough into the floodplain that it diverts flow from the main channel at all stages.

Study Site Description

We study the prevalence, distinguishing characteristics, and formation of floodplain channels within the state of Indiana using recently acquired state-wide airborne LiDAR. The two most recent periods of glaciation (pre-Wisconsinan and Wisconsinan) in Indiana have had an important effect on the landscape, as they have had in much of the USA and Canadian provinces that surround the Great Lakes. Pre-Wisconsinan glaciation(s) extended from the north (Gray and Letsinger, 2011), leaving part of the southern portion of Indiana unglaciated, whereas the maximum glacial extent during the Wisconsinan left the southern one-third of the state unglaciated (Figure 2). Glaciation in Indiana has created four different physiographic zones, which are broadly related to either glaciated or non-glaciated terrain. The physiographic zones related to glaciation include: the Northern Moraine and Lake Region, the Maumee Lake Plain Region, and the Central Till Plain. The unglaciated portion of Indiana is comprised of the Southern Hills and Lowland Region (Gray, 2000). For the purposes of this study, we simplify these physiographic zones into glaciated or unglaciated regions.

This distinction is important because glaciated terrain surrounding the Great Lakes has thicker Quaternary sediment cover in river valleys compared to more deeply incised and confined valleys in unglaciated regions. As glaciers retreated, sediment deposition from glacial outwash created low-relief till-plains, lacustrine deposits, and moraines (Gray, 2000). The thick sediment cover left by retreating glaciers in northern Indiana allows rivers and floodplains to function without much bedrock influence in relatively unconfined river valleys. The southern portion of Indiana has remained unglaciated. The unglaciated portion is characterized by heavily dissected uplands. Bedrock geology of southern Indiana is comprised of sandstones and a shoaling sequence of limestones in the central portion, siltstone to the east, and shale to the west. Rivers and floodplains in southern Indiana have more bedrock influence in their systems than their northern counterparts.

Methods

Datasets

We used the digital elevation model (DEM) derived from airborne LiDAR to map floodplain channels throughout Indiana. The airborne LiDAR data used in this study were acquired by the state over a three year period from 2011 to 2013 (http://www.indianamap.org). The post-processed bare-earth DEM was created by the state of Indiana by down sampling the data and averaging all bare-earth points within 1.5 m × 1.5 m bins. The horizontal coordinate system is North American Datum

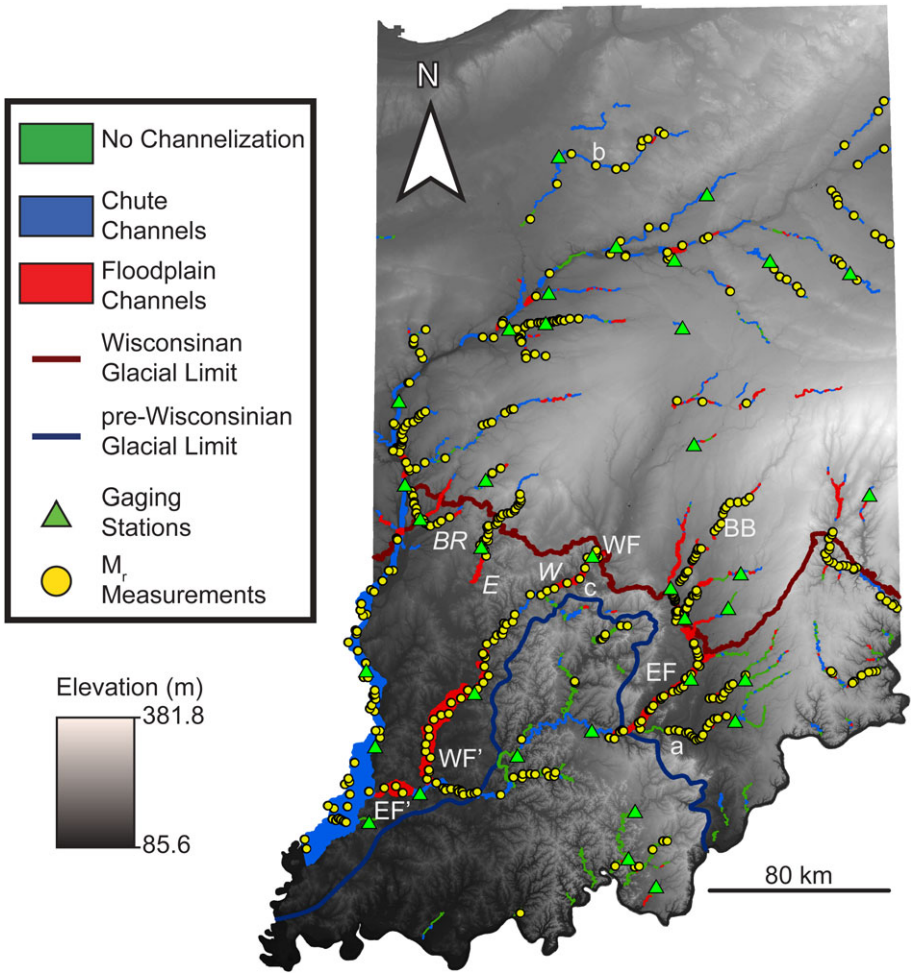

Figure 2. A 1.5-m shaded relief elevation model of Indiana showing floodplains characterized by different channelization types (note floodplain polygons widths are exaggerated for visualization), glacial limits, USGS stream gages used, and locations where meandering rate (M_r) data (Robinson, 2013) were available. Letters a, b, and c mark the locations of the floodplain types in Figure 4. Transects from WF to WF′ and EF to EF′ for the West Fork White River and East Fork White River, respectively are displayed in Figures 8 and 9. BR, E, and W are the locations of Big Raccoon Creek, Eel, and West Fork of the White River, respectively, used in the floodplain channel analysis displayed in Figure 11. BB is the location of the Big Blue River in Figure 12. [Colour figure can be viewed at wileyonlinelibrary.com]

1983 and the vertical datum is North American Vertical Datum 1988. The vertical accuracy of the LiDAR derived DEM is constrained by a maximum error range of ±15 cm.

Geomorphic data was also obtained on the main channels occupying the floodplains. Polygon data tracing the river banks (http://www.indianamap.org), originally utilized for DEM hydro-flattening, were used to calculate channel geometry. River polygons are available for ~85% of floodplain area mapped in this study. Though the coverage is not complete, the available river polygons are evenly distributed throughout the state and among the floodplains we mapped, suggesting that the river polygons suitably represent the population of floodplains in our dataset.

The statewide LiDAR elevation data was augmented with five additional data sets: aerial imagery, SSURGO national soil database (NRCS, 2015), 30 m resolution land cover data (Fry *et al.*, 2011), stream gage data from the US Geological Survey (USGS), and recent channel migration rate (M_r) (Robinson, 2013). Aerial imagery data were obtained from Google Earth (1 m resolution) and the Landsat 7 satellite (30 m resolution; http://landsatlook.usgs.gov/viewer.html). Infrared Landsat 7 images were compiled to view floodplains during flood stage. Soil and land cover data for the entire state were used to explore relationships between soil composition, land use, and floodplain topography. The M_r data were taken from Robinson (2013), who measured migration rates for 970 meander bends at select locations on 41 rivers in Indiana using historical imagery from ~1998 to 2011 in Google Earth. The frequency and magnitude of peak flooding events were also analyzed at 36 USGS gauging stations from 1987 to 2014.

Floodplain mapping based on channelization type

For the purposes of this research, we mapped the channelization type on the floodplains for river channels greater than 20 m wide. A threshold of 20 m was chosen because that was the smallest channel size with floodplain features that could be resolved and analyzed. The analysis was limited to the lowest elevation floodplain surface, which excludes higher elevation terraces. The lowest elevation floodplain surfaces were manually traced in ESRI ArcGIS on a slope map that shows the terrace riser separating the lowest elevation floodplain from higher, older terraced floodplains (Figure 3). We also excluded straightened rivers and floodplains with suburban or urban development.

All floodplains were mapped into one of three channelization types. The first type is floodplains with no channelization ($n = 278$). These floodplains have topography that is relatively featureless with no clear evidence of meandering (Figure 4A).

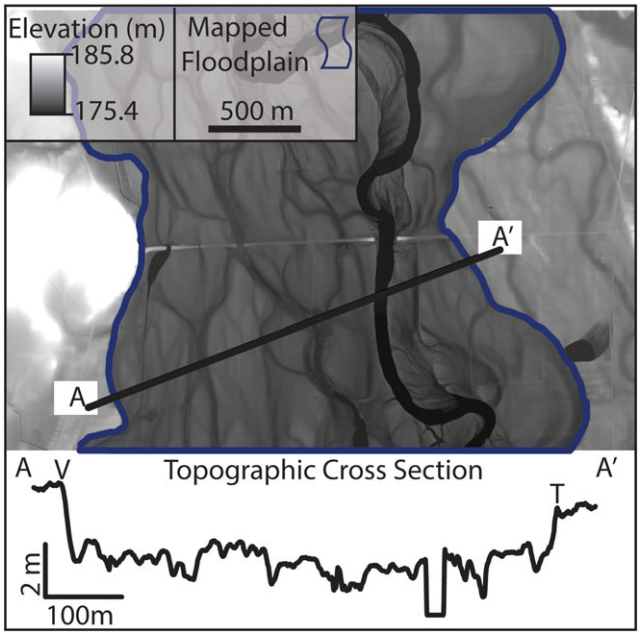

Figure 3. (A) For all rivers in this study we mapped the lowest elevation floodplain surface, defined in cross-section as a surface of relatively uniform elevation bordered by terrace risers (T) or valley walls (V). In this figure the mapped floodplain is marked in planview by the thick bold line. This example is from the East Fork of the White River valley, Indiana, USA. [Colour figure can be viewed at wileyonlinelibrary.com]

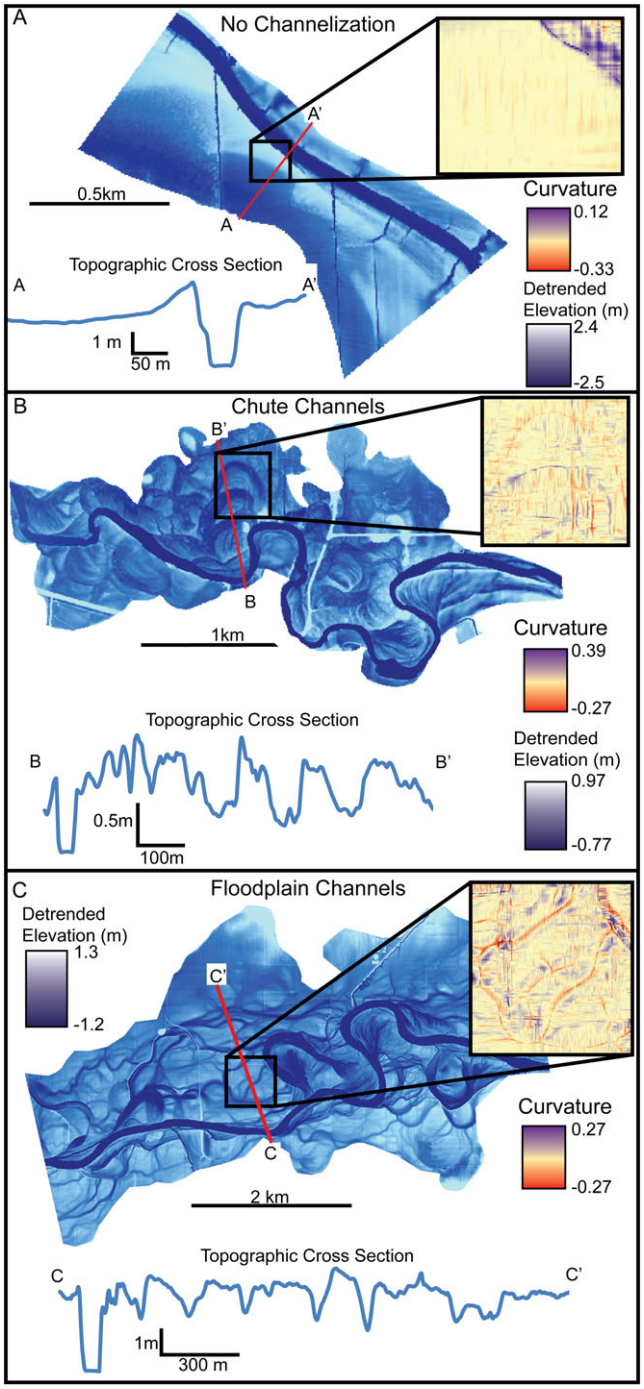

Figure 4. Digital elevation models (DEMs) of representative floodplains with different floodplain channelization types. The DEMs are detrended with their down-valley slopes. The locations of these examples are shown in Figure 2. Insets show the computed curvature map. [Colour figure can be viewed at wileyonlinelibrary.com]

The second type is floodplains with evidence of chute channels ($n = 498$). Chute channels are transient features, and we infer their existence by finding floodplains with features derived from chute channels, such as oxbow lakes (Figure 4B). These same features could be created by meander neck cutoffs and not chute channels. But, lower sinuosity rivers, like the ones studied here (sinuosity of ~1.2), tend to be dominated by chute cutoffs rather than neck cutoffs (Howard, 1996). Moreover, this is evident in the shape of the oxbows, where often the limbs of the oxbow are spatially separated suggesting a chute cutoff origin, rather than neck cutoff where the limbs would be touching. The third type is floodplains with floodplain channels ($n = 251$). Floodplain channels are recognized by finding channelized features in the floodplain that span more than one meander wavelength and are generally outside of the channel belt (Figure 4C). These floodplains, as we show later, may also have chutes channels because they are probably an important precursor to floodplain channel formation.

To clearly differentiate between these channelization types we transform the topographic data into curvature space. Curvature highlights the floodplain channels clearly (Figure 4). These maps were computed from a smoothed DEM (20×20 focal mean) to eliminate topographic noise. The curvature maps were computed using a cross-sectional curvature (CSC) method (Equation 1), where each cell of the DEM is computed using the neighboring cells as:

$$\mathrm{CSC} = 2\left(\frac{q^2 r - pqs + p^2 t}{p^2 + q^2}\right) \tag{1}$$

where,

$$p = \frac{\delta z}{\delta x}, q = \frac{\delta z}{\delta y}, r = \frac{\delta^2 z}{\delta x^2}, s = \frac{\delta^2 z}{\delta y \delta x}, t = \frac{\delta^2 z}{\delta y^2},$$

x and y are geographic coordinates (in meters), and z is elevation (in meters) (Jenness, 2013). Calculation of CSC computes negative values for convergent cells and positive values for divergent cells. Hence, curvature calculations aid in channel detection and determining if water would converge or diverge as it flows over a point. The curvature maps of floodplains with no channelization highlight levees (positive values flanking the channel) and tributaries entering the river, whereas the remainder of the floodplain shows no coherent trends in curvature values (Figure 4A). Floodplains with evidence of chutes (e.g. oxbows, and bar and chute cutoffs) show isolated channelized features (coherent negative trends; e.g. meander cutoffs) in the floodplain (Figure 4B). Floodplains exhibiting floodplain channels display long coherent trends of negative values in the curvature map (Figure 4C).

Floodplain binning and morphometrics

Mapped floodplains were discretized into 5-km long polygons. Geometric centerlines were computed for each floodplain polygon. Centerlines were generated by computing Thiessen polygons for each vertex along floodplain polygon edges (Smith and Cromley, 2012) and extracting the contiguous portions of the Thiessen polygons to produce floodplain centerlines. Sensitivity analysis shows that the metrics and statistics are insensitive to the discretization size choice. For some analyses we created more finely discretized floodplains; but unless otherwise stated, the discretization applied was 5-km.

We computed floodplain morphometrics from the DEM for each 5-km polygon. For each polygon we calculated characteristic floodplain width ($\mathrm{Fp_w}$), characteristic river width (R_w), characteristic floodplain slope (S_{fp}), and the river sinuosity (SI). The values for $\mathrm{Fp_w}$ and R_w were computed by dividing the floodplain and river polygon area by their respective centerline length. The S_{fp} value was computed by differencing the floodplain elevation of each endpoint and dividing by the centerline length. Sinuosity of the river channel was computed by dividing the river centerline length by the floodplain centerline length.

Where available, M_r measurements, land cover classes, surficial SSURGO data, and the number of overbank floods that occurred at USGS gages from 1987 to 2014 were compiled for each floodplain polygon. The M_r data were available for floodplain polygons classified as having no channelization ($n = 29$), chutes ($n = 134$), and floodplain channels ($n = 104$) (Figure 2). The M_r values were averaged if more than one value was located in a given polygon. Land cover data were analyzed by calculating the areal proportion in each floodplain polygon. The land cover classes differentiated between broad land-use categories (e.g. forested, cultivated land). We also calculated the areal proportion of the particle size modifier class of surficial SSURGO soil data to compare the distribution of soil composition among floodplain polygons.

We also directly measured the magnitude and frequency of flooding from the peak annual stream discharges at 35 USGS gaging stations from 1987 to 2014. Floodplains with no channelization, chute channels, and floodplain channels had 8, 21, and 6 gaging stations (Figure 2). For this measurement, flood stage is defined as the characteristic minimum elevation of the levee crests within a 100-m radius of the gage station. Our definition of flood stage agrees with flood stage datums reported by the National Weather Service for each river (http://water.weather.gov/ahps/). The flood magnitude is defined as the peak stage for a given flood event. A flood event is defined as a rise and fall of the water level from below bankfull stage to peak stage back to below bankfull. Individual flood events must be separated by a time interval on order of weeks to avoid double counting high frequency fluctuations.

Results

In total, we mapped 3064 $\mathrm{km^2}$ of floodplains (Figure 2) and found that floodplains with no channelization, chutes, and floodplain channels comprise 6.8%, 55.9%, and 37.3% of the total area, respectively. If normalized by floodplain length floodplains with no channelization, chutes, and floodplain channels account for 26.3%, 49.4%, and 24.3%, respectively, where the total length of mapped floodplains is 3388 km (Table I). Comparing distribution of floodplain types by area and by length underscores that floodplains with no channelization tend to be narrow and occupy a smaller proportion of the total area but a relatively large proportion of the total length, whereas floodplains with floodplain channels tend to be wide.

Characteristics of floodplains with different channelization types

Analysis for the 5-km polygons reveals interesting differences among floodplains with different channelization types. Floodplain channels have mean $\mathrm{Fp_w}$ that is approximately four times larger than those with no channelization and approximately two times larger than those with chute channels. Additionally, the mean $\mathrm{Fp_w}$ to R_w ratio is significantly different among types. Floodplains containing floodplain channels have a mean $\mathrm{Fp_w}/R_w$ that is nearly three times greater than the mean $\mathrm{Fp_w}/R_w$ of

Table I. Morphometric values for each of the floodplain channelization types

Floodplains with	Percent by length	Percent by area	Mean Fp_w (m)		Mean R_w (m)		Mean Fp_w/R_w		Mean S_{fp}		Mean SI		Mean M_r (m/yr)	
			+319.6		+60.8		+8.1		+0.003		+0.2		+0.3	
No Channelization	26.3	6.8	162.4	–82.6	39.2	–25.3	4.4	–2.4	0.0006	–0.0002	1.1	–0.1	0.0	–0.0
			+995.2		+108.3		+16.3		+0.002		+0.2		+3.0	
Chute Channels	49.4	55.9	381.1	–145.9	56.2	–29.1	8.5	–4.4	0.0006	–0.0002	1.2	–0.2	0.0	–0.0
			+1701.2		+86.8		+38.9		+0.002		+0.3		+3.0	
Floodplain Channels	24.3	37.3	697.9	–286.3	48.9	–27.6	20.4	–10.7	0.0008	–0.0003	1.4	–0.3	1.8	–1.8

Note: The data used for computing the mean and error shown is derived from the 5-km discretized polygons from the statewide mapping. The mean and one standard deviation (± values in the table) are computed by normalizing the data using a log transformation. The log normal standard deviation is subtracted from the log normal mean then transformed back into its original form, which is why the reported error is not symmetrical.

floodplains with chutes and five times greater than the mean Fp_w/R_w of floodplains with no channelization (Table I). There are no statistically significant differences in S_{fp} for the different floodplain types (p-value =0.1).

Soil data analysis reveals that floodplains with no channelization contain more silty soils than those containing chutes and floodplain channels (Figure 5). Floodplains with chute channels contain less silty loamy and clayey soil and have more sandy loamy soil than floodplains with floodplain channels.

Land cover analysis shows that floodplains with no channelization contain more forested land compared to those with chutes and floodplain channels, both of which are dominated by agricultural land uses (Figure 5).

There is evidence that the main river channel associated with different floodplain channelization types behaves differently. For instance, the main channels for floodplains with floodplain channels tend to have greater M_r relative to other types, especially those with no channelization where the channels are inactive (Table I). The differences in M_r values are also expressed in the sinuosity data, where the rivers of floodplains with no channelization have the lowest sinuosity and rivers with floodplain channels have the highest sinuosity.

Flooding frequency analysis of 26 years of stage data show that floodplains with no channelization reach bankfull discharge the least frequently, whereas floodplains containing floodplain channels reach bankfull discharge the most frequently (Figure 6). However, floodplains with floodplain channels are characterized by more shallow flooding depths than the other two types.

Of all variables in Table I, the ratio Fp_w/R_w changes the most as a function of floodplain channelization type. This is revealed more clearly when floodplains are plotted in the non-

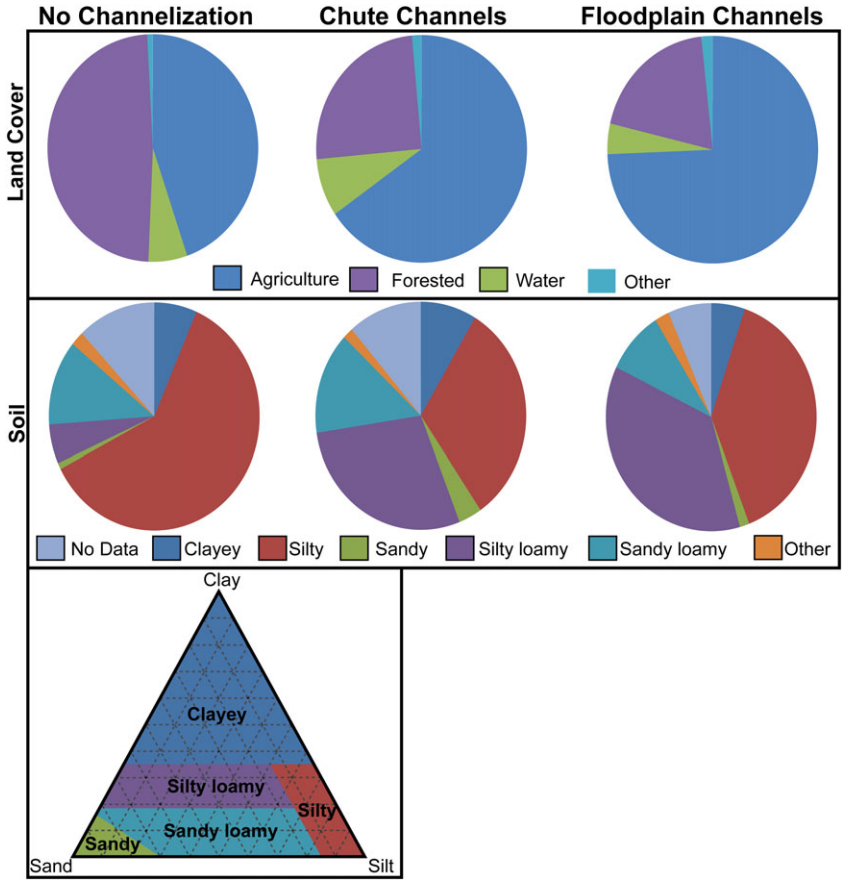

Figure 5. Land cover data shows floodplain channels are associated with an increasing amount of agriculture and a decreasing amount of forested land. Soil data show floodplains with floodplain channels and chutes contain less silty soil and more loamy soil than those with no channelization. The triangle shows the range of compositions of the various soil types displayed in the pie charts. [Colour figure can be viewed at wileyonlinelibrary.com]

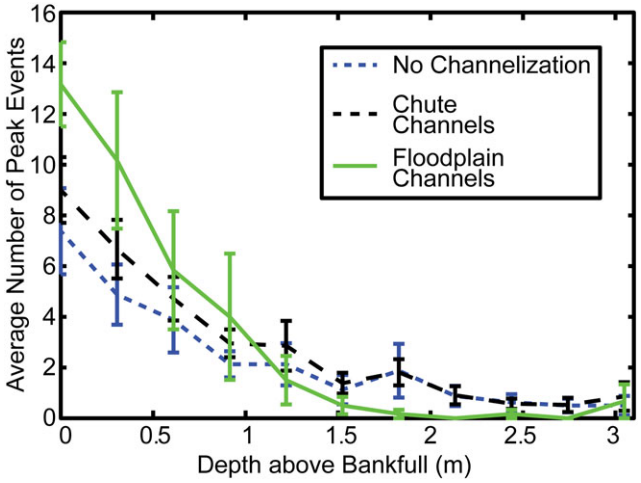

Figure 6. Average number of times per stream gage a given peak flooding depth has occurred for floodplains with different channelization types from 1987 to 2014. Error bars show the standard error. [Colour figure can be viewed at wileyonlinelibrary.com]

dimensional parameters space of Fp_w/R_w and S_{fp} (Figure 7). We statistically define the breaks between floodplains with different chute types on Figure 7 using a Fisher linear discriminant analysis (McLachlan, 2004). To determine the goodness-of-fit we calculated Matthews correlation coefficients (MCC) for each line. A MCC can range from −1 to 1, where 1 indicates the model perfectly predicts the data, 0 states the model does no better than a random prediction, and −1 states the model is in total disagreement with the dataset (Matthews, 1975). The MCC computed for the predicted separation of no channelization and chutes is 0.45, and the MCC for the separation of chutes and floodplain channels is 0.41. The separation line between no channelization and chute channels is nearly vertical suggesting S_{fp} has little control on their development (Figure 7). However, the slope of the separation line between floodplains with chute channel and floodplains with channels suggests some degree of S_{fp} control in that part of parameter space.

Reach-scale analysis of floodplain channelization

The floodplains of individual river systems can contain multiple types of channelization. Here we provide a more detailed analysis (using a 2-km discretization) of the floodplain types for the East Fork and the West Fork of the White River in Indiana (see Figure 2).

The East Fork of the White River displays all three floodplain channelization types over a 246 km reach (Figure 2, EF to EF′; Figure 8). The floodplain channels on this river are some of the best developed in terms of number of channels and continuity in a downstream direction. The presence of floodplain channels persists from 0 km to 25 km, but then abruptly changes to only chute channels at 25 km (Figure 8). This change in floodplain channelization type spatially correlates with changes in the measured morphometrics: S_{fp} and Fp_w/R_w abruptly decrease, at a transition consistent with discriminant analysis in Figure 7. At ~143 km the floodplain transitions from having chute channels to no channelization with no obvious morphometric differences. At ~173 km the floodplain transitions from having no channelization to containing chute channels, accompanied by an increase of Fp_w/R_w. At ~226 km the floodplain transitions back into having floodplain channels, where Fp_w/R_w, SI, and M_r also increase, while S_{fp} remains constant (Figure 8).

The floodplain of the West Fork of the White River predominantly contains chute channels and floodplain channels over a 144-km stretch (Figure 2, WF to WF′; Figure 9). Floodplain channels are prevalent from 0 km to ~25 km where it transitions to having only chutes. This transition correlates with a decrease in Fp_w/R_w and M_r, consistent with the transition noted on the East Fork of the White River (Figure 8). From ~53 km to ~75 km, the floodplain varies between containing chute channels and floodplain channels. Throughout these floodplains, the only evident difference, morphometrically, is that reaches with floodplain channels have a higher Fp_w/R_w. At ~89 km, the floodplain abruptly transitions from containing floodplain channels to chutes. At this transition there is a large decrease in Fp_w/R_w and M_r. At ~95 km the floodplain transitions back into exhibiting floodplain channels coincident with a large increase in Fp_w/R_w, SI, and M_r.

Analysis of floodplain channels

To understand the geometric attributes of floodplain channels in more detail, we conducted analyses of the floodplain channels to determine their basic geometric character and their origin. For this analysis we focused on the well-developed floodplain channels on West Fork of the White River, Eel River, and Big Raccoon Creek, Indiana (Figure 2).

Analysis of aerial imagery reveals distinct differences among reaches of floodplain channels. Many of the floodplain channels are spatially associated with relict scroll bars. These scroll bars are visible in the 1.5-m LiDAR DEM and historical images. For instance, satellite images of the Eel River highlight relict

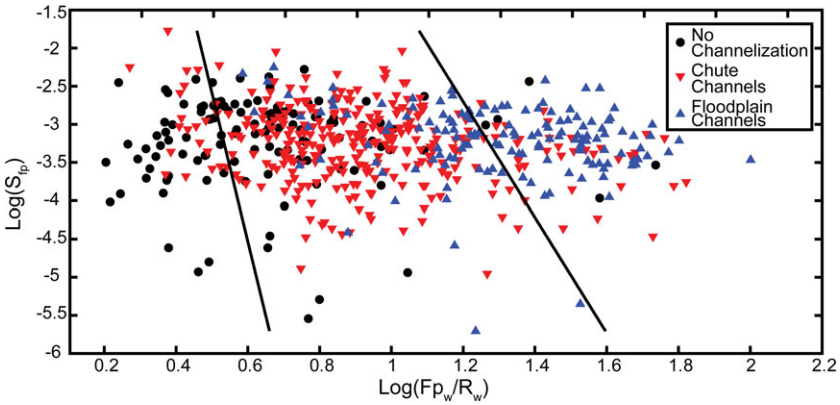

Figure 7. Non-dimensional parameter space illustrating clustering of floodplains with different channelization types. Solid lines are the class divisions from a Fisher linear discriminant analysis, demonstrating chutes and floodplain channels have different floodplain slopes (S_{fp}) and the floodplain-to-river width ratio (Fp_w/R_w). [Colour figure can be viewed at wileyonlinelibrary.com]

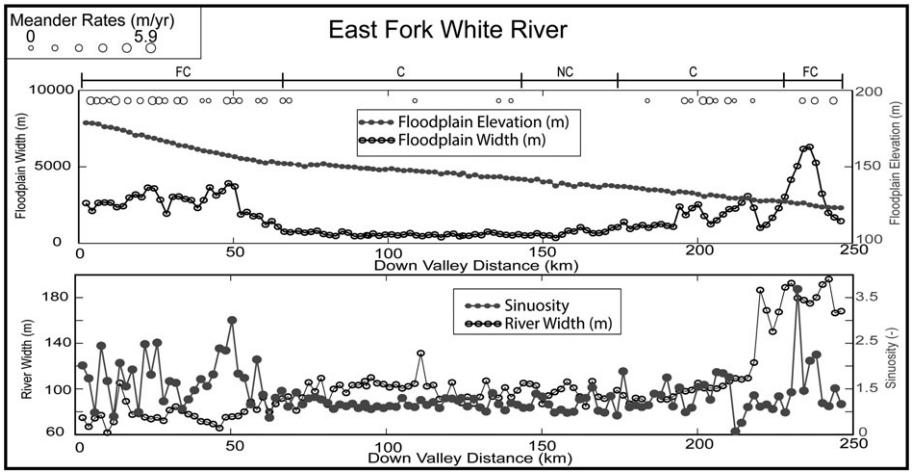

Figure 8. Down-valley plot for East Fork of the White River showing how floodplain morphometrics vary with respect to changing floodplain channelization types (indicated as NC, C, and FC above the top plot for no channelization, chute channels, and floodplain channels, respectively). The location of the reach is marked on Figure 2 as EF–EF′.

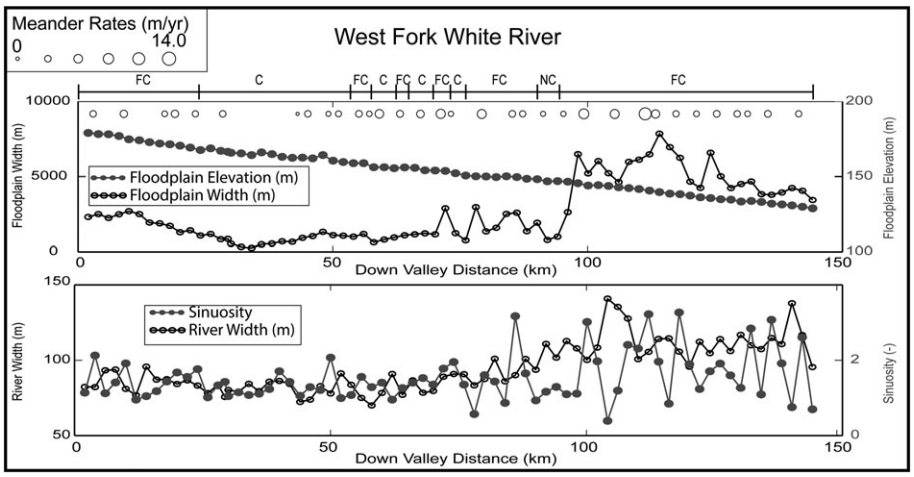

Figure 9. Down-valley plot for West Fork of the White River showing how floodplain morphometrics vary with respect to changing floodplain channelization types indicated as NC, C, and FC above the top plot for no channelization, chute channels, and floodplain channels, respectively).The location of the reach is denoted on Figure 2 as WF–WF′.

scroll bars, which show up nicely because of differences in soil properties (Figure 10).

Based on this association we mapped the floodplain channels into two components: those channel segments associated with scroll-bar deposits and those that are not. We classify channel segments as being associated with scroll bars when the channel segment is found on the outer edge of these scroll bars and the channel has a planform shape that is conformable to the scroll bars (green channels in Figure 10). Based on their association with scroll bars, we suggest these channel segments were once part of the main channel and created from meander cut-offs. The remaining channelized features are not clearly associated with scroll bars because their planform shape does not conform to the scroll bar shape and in some cases these channels cut across scroll bars (red channels in Figure 10). We refer to the remaining channel segments that are not spatially associated with scroll bars as secondary channels.

Mapping these two components of floodplain channels reveals that floodplain channels are composed of meander cutoffs linked together by secondary channels (Table II; Figure 11). For instance, what can appear to be long, continuous down-valley channels in LiDAR elevation data are actually a series of meander cutoffs connected together by secondary channels (Figure 11). On Big Raccoon Creek, Eel River, and West Fork of the White River, meander cutoffs account for 71%, 73%, and 48% of the total channelized floodplain length, respectively (Table II).

To further explore the hypothesis that floodplain channels are composed of two genetically different components, we analyzed the channel width, bankfull depth, and slope of each component. Floodplain channel segments classified as meander cutoffs are on average wider and deeper and have a larger width-to-depth ratio than secondary channels. Meander cutoff segments have a width more similar to their main channel, whereas secondary channels are commonly much narrower than the main channel (Table II). This is broadly consistent with the interpretation that the channel segments associated with scroll bars (i.e. the meander cutoffs) are remnants of the main channel.

Discussion

We found that floodplains with different channelization types have different morphometrics. Floodplains with no channelization are characterized by their relatively narrow Fp_w, low Fp_w/R_w, and stationary river channels. Floodplains containing chute channels tend to have higher M_r, and an intermediate Fp_w compared to the other floodplains. Floodplains exhibiting

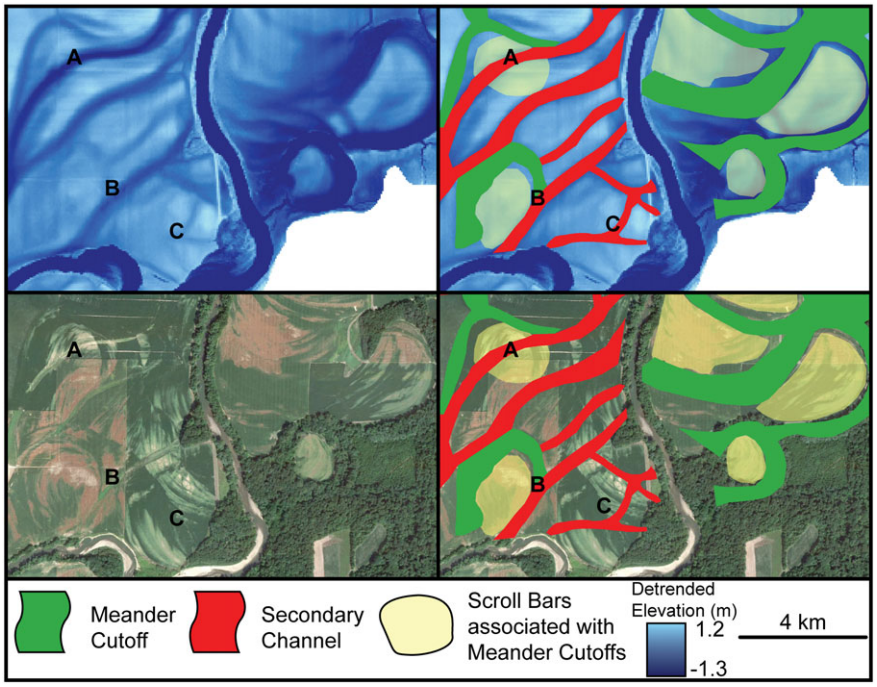

Figure 10. The two images on the left show a 1.5 m digital elevation model (DEM) (upper) and corresponding Google Earth image (lower). Note that relict scroll bars are clearly visible in the image and more obscure in the DEM. The right half of the figure shows the interpreted channels, where green indicates meander cutoff and red indicates secondary channels. The letters A, B, and C highlight locations where secondary channels cut across scroll bars associated with meander cutoffs, secondary channels link up to meander cutoffs, and secondary channels cut through recent scroll bars (not associated with meander cutoffs), respectively. The images above are for the Eel River, Indiana, USA, noted on Figure 2 (E). [Colour figure can be viewed at wileyonlinelibrary.com]

Table II. Morphometrics for the mapped secondary channels and meander cutoffs for the Big Raccoon River, Eel River, and West Fork of the White River

Location	Average R_w (m)	Channel type	Per cent by length	Per cent by area	Mean width (m)		Mean maximum depth (m)		Mean width/ depth (m/m)		Mean slope (m/m)	
						+46.9		+1.4		+59.5		+0.003
		Meander cutoff	71	75	34.7	–25.6	0.9	–0.5	39.9	–20.0	0.0009	–0.0003
						+36.0		+1.5		+56.9		+0.003
Big Raccoon	27.5	Secondary	29	25	26.8	–20.0	0.8	–0.4	33.5	–19.8	0.0009	–0.0003
						+62.1		+2.4		+53.8		+0.002
		Meander cutoff	64	73	44.2	–31.4	1.4	–0.8	31.9	–18.9	0.0007	–0.0002
						+41.9		+2.3		+40.5		+0.004
Eel	39.2	Secondary	36	27	29.2	–20.3	1.4	–0.8	21.6	–11.6	0.001	–0.0003
						+74.8		+2.6		+56.2		+0.002
		Meander cutoff	48	67	48.9	–31.9	1.5	–0.8	33.7	–20.2	0.0008	–0.0003
						+38.0		+2.0		+49.0		+0.004
West Fork White	83.2	Secondary	52	33	25.7	–17.4	1.1	–0.6	24.3	–12.1	0.001	–0.0003

Note: The mean and one standard deviation (error shown) is computed by normalizing the data from each polygon using a log transformation, similar to Table I. The mean maximum depth in the table represents the highest elevation of the meander cutoff or secondary channel in each polygon subtracted from the lowest point in each polygon; the distribution of polygons is then averaged.

floodplain channels characteristically have the highest M_r, and Fp_w. Morphometric and mapping analysis of floodplain channels reveals they are comprised of secondary channels linking together meander cutoffs.

What processes create floodplain channels?

The data from this study suggest that floodplain channels arise through incisional processes rather than progradational or depositional processes. Progradational channels, like the Saskatchewan River in the Cumberland Marshes (Smith *et al.*, 1989; Farrell, 2001), tend to form on low gradient floodplains (Hajek and Edmonds, 2014) where water ponds during floods. However, in our dataset, floodplains containing floodplain channels are steeply sloped compared to progradational systems (Hajek and Edmonds, 2014). Moreover, there is no visible geomorphic evidence for progradational avulsions, such as crevasse splay (Farrell, 2001). There is also no evidence that the floodplain channels in this study are part of broad features of positive relief created from deposition.

Instead, we suggest that floodplain channels form when preexisting channel segments (meander cutoffs) are connected together by secondary channels. The secondary channels generally post-date the meander cutoffs in most floodplains because they often cut across scrolls bars or link them together (Figure 10). This linking process could occur during flood stage where the presence of a meander cutoff on the floodplain creates local flow acceleration (as flow enters a deeper portion of the floodplain) and knickpoints moves upstream until they

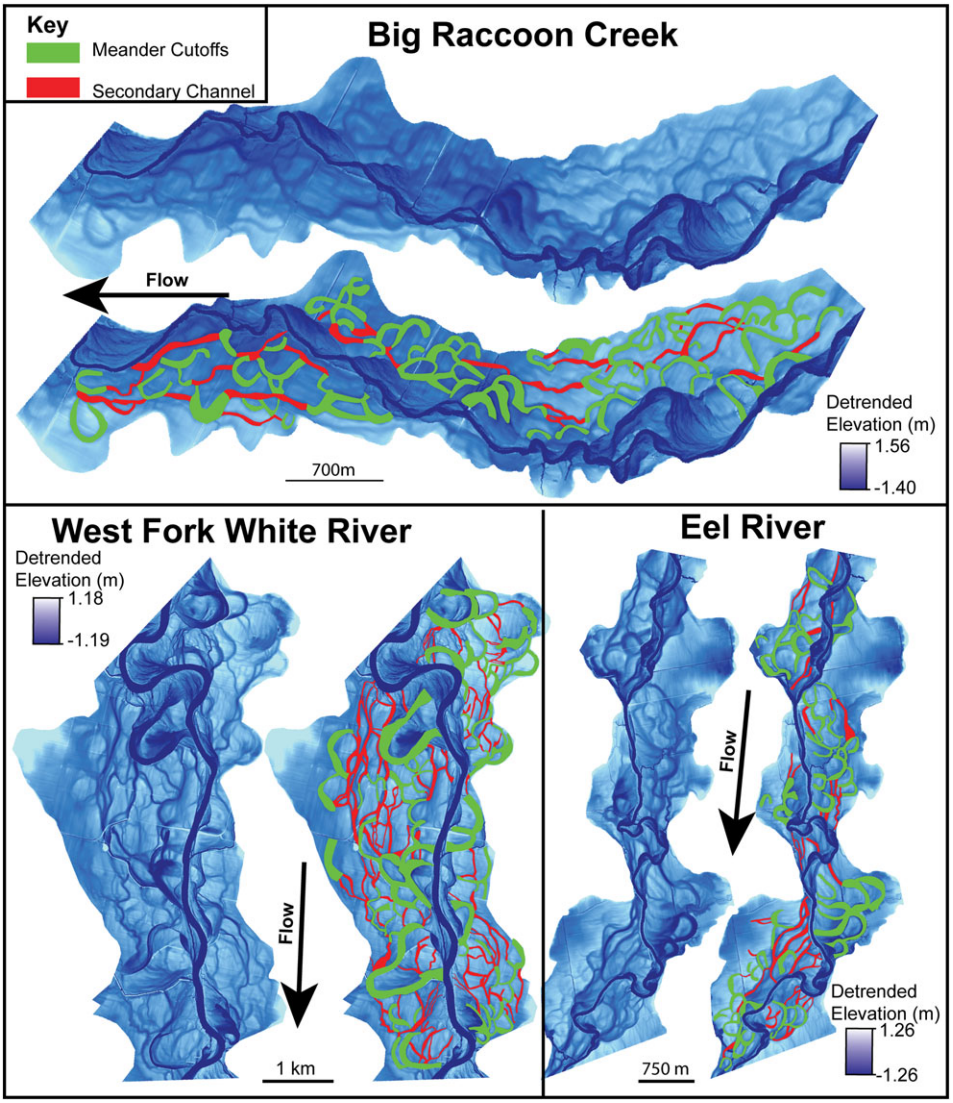

Figure 11. Floodplain channel mapping for three different floodplains. Green polygons indicate meander cutoffs and red polygons are secondary channels. Locations of Big Raccoon Creek, Eel River, and West Fork of the White River are shown on Figure 2 as BR, E, and W, respectively. [Colour figure can be viewed at wileyonlinelibrary.com]

diffuse or connect with another meander cutoff or secondary channel (e.g. Miller, 1991).

Relevant modeling results from Hajek and Edmonds (2014) show that the presence of pre-existing floodplain topography can accelerate overland flow and create erosive floodwaters during flood events. In their models, the locus of erosion enlarges, collecting more overland flow, thereby increasing erosion. Eventually the scour point enlarges and functions as a knickpoint that erodes upstream into the floodplain. The process described by Hajek and Edmonds (2014) and our proposed process for floodplain channels is similar to that of chute channels, which form through headward incision and knickpoint migration (up valley) as flow plunges back into the river channels (Keller and Swanson, 1979; Gay *et al.*, 1998; Thompson, 2003). The extent to which these secondary channels arise from the same processes as chute channels remains an open question.

What controls the occurrence of floodplain channels?

Our mapping (Figures 10 and 11) suggests that two important processes are required to create floodplain channels: (1) meander cutoffs, and (2) secondary channels that link the cutoffs together. Here we explore the extent to which floodplains with floodplain channels are actually dominated by these processes.

Production of meander cutoffs is positively correlated with channel migration rate, channel sinuosity, and sediment supply (Constantine and Dunne, 2008; Constantine *et al.*, 2014). The main channels in floodplains with floodplain channels have the highest sinuosity and average rates of meander migration (Table I), suggesting they produce more cutoffs than other floodplains. Constantine *et al.* (2014) found that high rates of sediment supply increased production of meander cutoffs. Though we do not have measurements of sediment supply, the floodplains in our dataset with floodplain channels often occur near the position of the last glacial maximum in Indiana (Figure 1), and these systems probably received larger sediment supplies during deglaciation when meandering channels formed in these river valleys.

Relative floodplain width is also an important controlling variable that promotes floodplain channels (Figure 7). Wide floodplains allow the main channel to freely meander, which increases channel migration rate, something we see in our dataset (Table I). Even so, for a given sinuosity and cutoff frequency, wider floodplains still would be advantageous for floodplain channel formation because meander cutoffs would be distributed over a larger area. This would provide space between cutoffs for secondary channels to link these meander

cutoffs together and form floodplain channels. On narrower floodplains, meander cutoffs would be more densely spaced, possibly suppressing the process of secondary channel formation that nucleates off meander cutoff segments forming floodplain channel.

If secondary channels are formed through incisional processes, as we suggest, than some floodplain erosion probably occurs during flood. Floodplains with floodplain channels flood most frequently (Figure 6), possibly producing the most geomorphic work on the floodplain (Wolman and Miller, 1960). However, it is difficult to isolate flooding frequency as a cause of the floodplain networks rather than an effect. Floodplain channels are most often found in floodplains with a large proportion of non-cohesive soil and cultivated land (Figure 5). The lack of vegetation on cultivated floodplains allows flood waves to flow unimpeded potentially increasing shear stress on the bed. Finally, floodplains with floodplain channels tend to have sandier soils (Figure 5), which all else being equal should make the surface easier to erode by flood waters compared to more densely vegetated muddy floodplains (Konsoer *et al.*, 2016).

To what extent is the occurrence of floodplain channels related to the Wisconsinan glaciation?

There is some correspondence between the position of floodplain channels in our study and the spatial extent of the Wisconsinan glaciation in Indiana (Figure 2). A reasonable null hypothesis for the origin of floodplain channels is that they are the annexed relicts of the glacial braided streams that formerly occupied these valleys (Fraser, 1994).

Data constraining the formation age of the floodplain channels would be a strong test of this idea, but in the absence of those data we have three lines of evidence to support the hypothesis that floodplain channels are probably not the annexed relicts of glacial streams. First, there are surficial deposits on higher, older terraces that more strongly resemble braided stream morphology than the floodplain channels we mapped. For example, the floodplain of the Big Blue River near Shelbyville, Indiana (Figure 12) contains floodplain channels, whereas the higher terrace adjacent to the floodplain has a significantly different, braided surficial morphology. The terrace's surficial morphology shows a large compound bar with a teardrop shape similar to bar shapes in braided rivers (Kelly, 2006; Schuurman *et al.*, 2013). The channels on the terrace are wider than the main channel on the modern floodplain and contain no evidence for scroll bar deposition. Second, cross-cutting relationships suggest secondary channels in floodplain networks post-date the onset of meandering in these valleys. There is ample evidence that secondary channels cut across meander cutoffs and are sometimes orthogonal to scroll bars (Figures 10 and 11). Third, meander cutoffs can be found at the margins of most floodplains exhibiting floodplain channels (Figure 4C). This suggests that even if the modern floodplains are much older than we expect and were once braided, the meandering river has traversed the entire floodplain surface, likely reworking and possibly eliminating paleo-braided channel morphologies if they did exist.

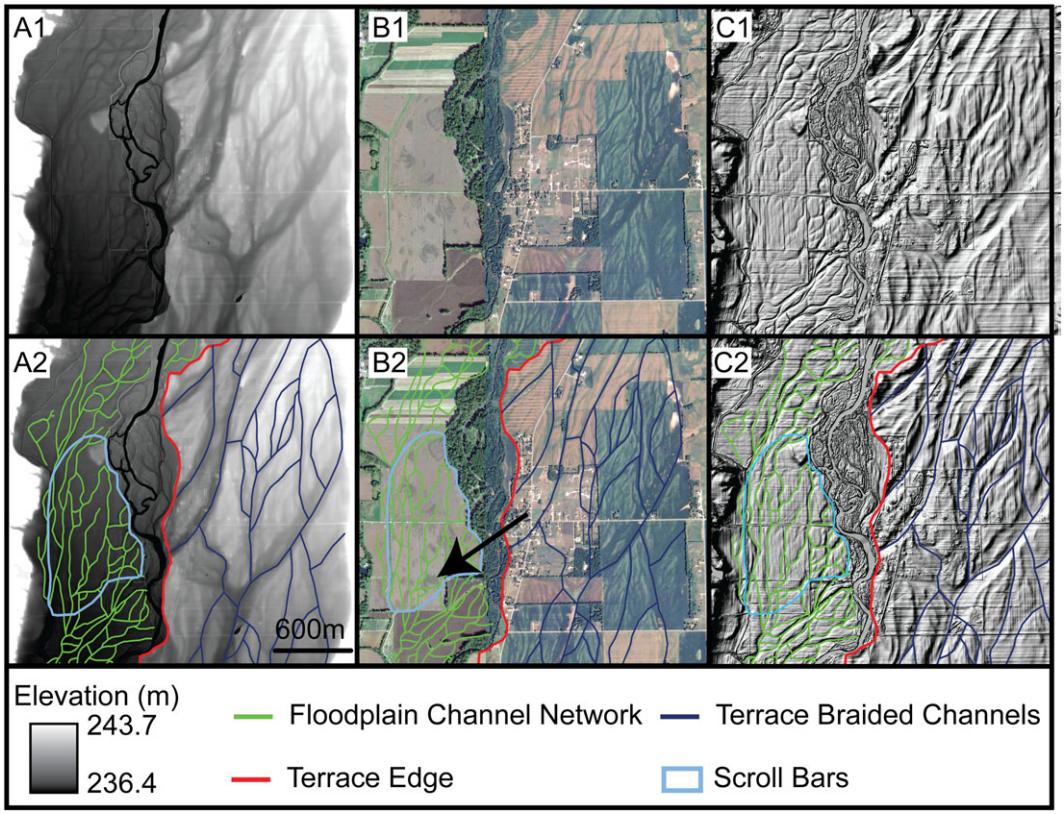

Figure 12. The top panel (A1–C1) shows the uninterpreted images and the bottom (A2–C2) shows interpretations. Images A, B, and C are the digital elevation model (DEM), Google Earth Imagery, and DEM hillshade with 5× vertical exaggeration of the Big Blue River. The DEM (A1 and A2) highlights that channels on the terraces are larger than those in the floodplain channel network. The Google Earth images (B1 and B2) show the presence of scroll bars, darker spots inside of light blue polygon as noted by the black arrow, in the floodplain and the lack of scroll bars on the terraces. The DEM hillshade (C1 and C2) accentuates the topographic variability along the floodplain and terrace. The location of these images is shown on Figure 2 as BB. [Colour figure can be viewed at wileyonlinelibrary.com]

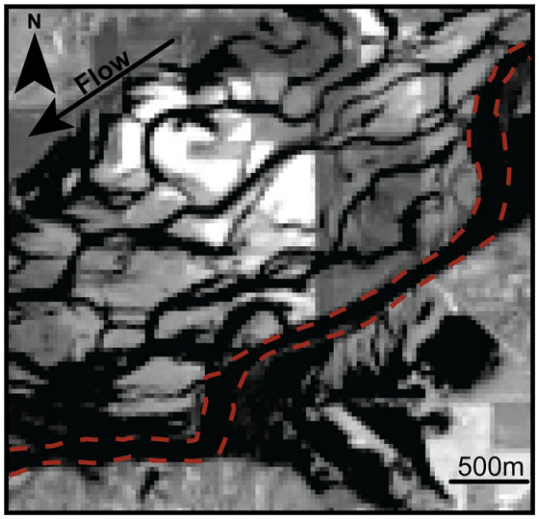

Figure 13. Landsat 7 (near infrared band) image of the White River near Paragon, Indiana, during flood on April 22, 2013. Black indicates water and the gray scale is land. The red dashed line outlines the edges of the river channel. [Colour figure can be viewed at wileyonlinelibrary.com]

Implications for floodplain morphodynamics

Our analysis suggests that floodplain channels are prominent throughout Indiana and possibly form through incisional processes. These channels have interesting implications for the long-term evolution of floodplain and the main river channel. One possibility is that these floodplain channels are part of the avulsion process. For instance, if a given floodplain channel pathway enlarges its cross-sectional area through time it may divert enough flow to cause a river avulsion. This is similar to the model proposed for incisional avulsions (Mohrig *et al.*, 2000; Slingerland and Smith, 2004; Hajek and Edmonds, 2014), but our work highlights how such an avulsion channel could form through the process of secondary channels connecting meander cutoffs.

Another possibility is that as the floodplain channels enlarge no avulsions occur, and instead the discharge will be shared among the channels. In this way floodplain channels would aid in the transition of river planform geometry from a single threaded system to a multi-channeled anabranching system (Miller, 1991; Nanson and Knighton, 1996; Latrubesse, 2008). Anabranching rivers consist of multiple river channels that share the water discharge at all river stages. Currently, there are no anabranching rivers in the area we mapped because the channels are single thread at stages up to bankfull. But, these floodplain channels have increased their cross-sectional area enough to function as anabranching when the water stage is above bankfull. For example, during a ~10-year flood on the White River near Paragon, Indiana, the channel appears anabranching since flood waters are confined to the floodplain channels, leaving the areas between the channels dry (Figure 13). The fluvial system may transition to anabranching if the floodplain channels continue to enlarge their cross-sectional area and convey flow at all stages.

Conclusions

Mapping and classification of 3064 km^2 of floodplains reveal there are three distinct floodplains with different types of channelization on floodplains in Indiana. In terms of area, we found that floodplains with no channelization account for 6.8%, floodplains with chutes account for 55.9%, and floodplains with channels account for 37.3%. If normalized by floodplain length the proportions change to 26.3%, 49.4%, and 24.3%, respectively, where the total length of mapped floodplains is 3388 km. Floodplains with no channelization (not including the main channel) are relatively featureless and are characterized by relatively narrow floodplain-to-river width ratios (Fp_w/R_w), river channels that have small migration rates, and reach bankfull discharge the least frequently. Floodplains with chutes channels are characterized by river channels that migrate, and an intermediate Fp_w/R_w. Floodplains with floodplain channels are characterized by river channels with highest rates of migration, the highest Fp_w/R_w, are dominated by agricultural land use and reach bankfull discharge frequently.

Our mapping of individual floodplains demonstrates that floodplain channels are composed of meander cutoffs linked together by secondary channels. In this way, meander cutoff production is a necessary but not sufficient condition for floodplain channel formation; the conditions that promote secondary channel formation are a promising area of future research.

The floodplain channels observed in this study may prove to have important implications for river avulsion and planform geometry of rivers. For instance, if a given floodplain channel enlarges enough it may cause an avulsion. In a similar view, if multiple floodplain channel pathways are enlarging, and the channels are stable, the current river channel could transition to an anabranching planform geometry.

Acknowledgements—SRD was supported by EAR 1249330. DAE would like to acknowledge support from NSF grant EAR 1249330 and to the Donors of the American Chemical Society Petroleum Research Fund for support (or partial support) of this research. The authors would like to thank reviews from Kory Konsoer, Christian Braudrick, and Joel Rowland, as well as comments from an anonymous reviewer.

References

Ashmore PE. 1991. How do gravel-bed rivers braid? *Canadian Journal of Earth Sciences* **28**: 326–341. DOI:10.1139/e91-030.

Bridge JS. 2003. Rivers and Floodplains: Forms, Processes, and Sedimentary Record. Blackwell: Malden, MA.

Braudrick CA, Dietrich WE, Leverich GT, Sklar LS. 2009. Experimental evidence for the conditions necessary to sustain meandering in coarse-bedded rivers. *Proceedings of the National Academy of Sciences* **106**(40): 16936–16941. DOI:10.1073/pnas.0909417106.

Camporeale C, Perona P, Porporato A, Ridolfi L. 2005. On the long-term behavior of meandering rivers. *Water Resources Research* **41**(12): W04109. DOI:10.1029/2005WR004109.

Constantine JA, Dunne T. 2008. Meander cutoff and the controls on the production of oxbow lakes. *Geology* **36**: 23–26. DOI:10.1130/G24130A.1.

Constantine JA, Dunne T, Ahmed J, Legleiter C, Lazarus ED. 2014. Sediment supply as a driver of river meandering and floodplain evolution in the Amazon Basin. *Nature Geoscience* **7**(12): 899–903. DOI:10.1038/NGEO2282.

Constantine JA, McLean SR, Dunne T. 2010. A mechanism of chute cutoff along large meandering rivers with uniform floodplain topography. *Geological Society of America Bulletin* **122**(5–6): 855–869. DOI:10.1130/B26560.1.

Dunne T, Aalto RE. 2013. Large River Floodplains. In Treatise on *Geomorphology*, John FS, Wohl EE (eds). Academic Press: San Diego, CA; 645–678.

Fagan SD, Nanson GC. 2004. The morphology and formation of floodplain-surface channels, Cooper Creek, Australia. *Geomorphology* **60**(1): 107–126. DOI:10.1016/j.geomorph.2003.07.009.

Farrell KM. 2001. Geomorphology, facies architecture, and high-resolution, non-marine sequence stratigraphy in avulsion deposits, Cumberland Marshes, Saskatchewan. *Sedimentary Geology* **139**(2): 93–150.

Fraser G. 1994. Sequences and sequence boundaries in glacial sluiceways beyond glacial margins. In Incised valley systems: Origin and

sedimentary sequences, Dalrymple R, Boyd R, Zaitlin B (eds), SEPM Special Publication 51. SEPM: Tulsa, OK; 337–351.

Fry J, Xian G, Jin S, Dewitz J, Homer C, Yang L, Barnes C, Herold N, Wickham J. 2011. Completion of the 2006 national land cover database for the conterminous United States. *Photogrammetric Engineering & Remote Sensing* **77**(9): 858–864.

Gay GR, Gay HH, Gay WH, Martinson HA, Meade RH, Moody JA. 1998. Evolution of cutoffs across meander necks in Powder River, Montana, USA. *Earth Surface Processes and Landforms* **23**(7): 651–662.

Gray HH. 2000. Physiographic Divisions of Indiana (No. 61). Indiana Geological Survey, Indiana University: Bloomington, IN.

Gray HH, Letsinger SL. 2011. A History of Glacial Boundaries in Indiana, Indiana Geological Survey Special Report 71. Indiana Geological Survey, Indiana University: Bloomington, IN; 10 pp.

Grenfell M, Aalto R, Nicholas A. 2012. Chute channel dynamics in large, sand-bed meandering rivers. *Earth Surface Processes and Landforms* **37**(3): 315–331. DOI:10.1002/esp.2257.

Hajek EA, Edmonds DA. 2014. Is river avulsion style controlled by floodplain morphodynamics? *Geology* **42**(3): 199–202. DOI:10.1130/G35045.1.

Harrison LR, Dunne T, Fisher GB. 2015. Hydraulic and geomorphic processes in an overbank flood along a meandering, gravel-bed river: implications for chute formation. *Earth Surface Processes and Landforms* **40**(9): 1239–1253. DOI:10.1002/esp.3717.

Hooke JM. 1995. River channel adjustment to meander cutoffs on the River Bollin and River Dane, northwest England. *Geomorphology* **14**(3): 235–253.

Howard AD. 1996. Modelling channel evolution and floodplain morphology. In Floodplain Processes, Anderson MG, Walling DE, Bates PD (eds). John Wiley & Sons: Chichester; 15–62.

Jenness JS. 2013. DEM Surface Tools for ArcGIS (surface_area.exe). Jenness Enterprises: Flagstaff, AZ.

Keller EA, Swanson FJ. 1979. Effects of large organic material on channel form and fluvial processes. *Earth Surface Processes* **4**(4): 361–380.

Kelly S. 2006. Scaling and hierarchy in braided rivers and their deposits: examples and implications for reservoir modelling. In Braided Rivers: Process, Deposits, Ecology and Management, Sambrook Smith GH, Best JL, Bristow CS, Petts GE (eds). Blackwell: Oxford; 75–106.

Konsoer KM, Rhoads BL, Langendoen EJ, Best JL, Ursic ME, Abad JD, Garcia MH. 2016. Spatial variability in bank resistance to erosion on a large meandering, mixed bedrock-alluvial river. *Geomorphology* **252**: 80–97.

Latrubesse EM. 2008. Patterns of anabranching channels: The ultimate end-member adjustment of mega rivers. *Geomorphology* **101**(1): 130–145.

Lewin J, Ashworth PJ. 2014. The negative relief of large river floodplains. *Earth-Science Reviews* **129**: 1–23.

Matthews BW. 1975. Comparison of the predicted and observed secondary structure of T4 phage lysozyme. *Biochimica et Biophysica Acta (BBA) – Protein Structure* **405**(2): 442–451.

McGowen JH, Garner LE. 1970. Physiographic features and stratification types of coarse-grained point bars: modern and ancient examples. *Sedimentology* **14**(1–2): 77–111.

McLachlan G. 2004. Discriminant Analysis and Statistical Pattern Recognition (Vol. **544**). John Wiley & Sons: Chichester.

Mertes LA, Dunne T, Martinelli LA. 1996. Channel–floodplain geomorphology along the Solimões-Amazon river, Brazil. *Geological Society of America Bulletin* **108**(9): 1089–1107.

Miller JR. 1991. Development of anastomosing channels in south-central Indiana. *Geomorphology* **4**(3): 221–229.

Mohrig D, Heller PL, Paola C, Lyons WJ. 2000. Interpreting avulsion process from ancient alluvial sequences: Guadalope-Matarranya system (northern Spain) and Wasatch Formation (western Colorado). *Geological Society of America Bulletin* **112**(12): 1787–1803.

Nanson GC, Knighton AD. 1996. Anabranching rivers: their cause, character and classification. *Earth Surface Processes and Landforms* **21**(3): 217–239.

Natural Resources Conservation Service (NRCS). 2015. Natural Resources Conservation Service, United States Department of Agriculture. Web Soil Survey. http://websoilsurvey.nrcs.usda.gov/ [14 January 2015].

Robinson BA. 2013. Recent (circa 1998 to 2011) Channel-migration Rates of Selected Streams in Indiana, Scientific Investigation Report, 5168. US Geological Survey: Reston, VA; 46.

Rust BR. 1981. Sedimentation in an arid-zone anastomosing fluvial system: Cooper's Creek, Central Australia. *Journal of Sedimentary Research* **51**(3): 745–755.

Rust BR, Legun AS. 1983. Modern anastomosing-fluvial deposits in arid Central Australia, and a Carboniferous analogue in New Brunswick, Canada. *Modern and Ancient Fluvial Systems, Special Publication of the International Association of Sedimentologists* **6**: 385–392.

Schuurman F, Marra WA, Kleinhans MG. 2013. Physics-based modeling of large braided sand-bed rivers: bar pattern formation, dynamics, and sensitivity. *Journal of Geophysical Research - Earth Surface* **118**(4): 2509–2527.

Slingerland R, Smith ND. 2004. River avulsions and their deposits. *Annual Reviews: Earth and Planetary Science* **32**: 257–285.

Smith MJ, Cromley RG. 2012. Measuring historical coastal change using GIS and the change polygon approach. *Transactions in GIS* **16**(1): 3–15.

Smith ND, Cross TA, Dufficy JP, Clough SR. 1989. Anatomy of an avulsion. *Sedimentology* **36**(1): 1–23.

Stølum HH. 1998. Planform geometry and dynamics of meandering rivers. *Geological Society of America Bulletin* **110**(11): 1485–1498.

Thompson DM. 2003. A geomorphic explanation for a meander cutoff following channel relocation of a coarse-bedded river. *Environmental Management* **31**(3): 0385–0400. DOI:10.1007/s00267-002-2842-0.

Trigg MA, Bates PD, Wilson MD, Schumann G, Baugh C. 2012. Floodplain channel morphology and networks of the middle Amazon River. *Water Resources Research* **48**(10). DOI:10.1029/2012WR011888.

van Dijk WM, Lageweg WI, Kleinhans MG. 2012. Experimental meandering river with chute cutoffs. *Journal of Geophysical Research: Earth Surface* **117**(F3). DOI:10.1029/2011JF002314.

Wolman MG, Miller JP. 1960. Magnitude and frequency of forces in geomorphic processes. *The Journal of Geology* **68**(1): 54–74.

Zinger JA, Rhoads BL, Best JL. 2011. Extreme sediment pulses generated by bend cutoffs along a large meandering river. *Nature Geoscience* **4** (10): 675–678. DOI:10.1038/ngeo1260.